# Theoretical study on the optimal thermal excitation of bimaterial cantilevers

Vinh N.T. Pham[1], Chu Manh Hoang[2], Ho Thanh Huy[3], Le Tri Dat[4,5], Nguyen Duy Vy[4,5,*], Takuya Iida[6,7], and Amir Farokh Payam[8]

[1]*Department of Physics, Ho Chi Minh City University of Education, Ho Chi Minh City, Vietnam*
[2]*International Training Institute for Materials Science, Hanoi University of Science and Technology, Hanoi 10000, Vietnam*
[3]*Department of Physics and Engineering Physics, Ho Chi Minh City University of Science, VNU-HCM, Vietnam*
[4]*Laboratory of Applied Physics, Advanced Institute of Materials Science, Ton Duc Thang University, Ho Chi Minh City, Vietnam*
[5]*Faculty of Applied Sciences, Ton Duc Thang University, Ho Chi Minh City, Vietnam*
[6]*Department of Physical Science, Osaka Prefecture University, Sakai 599-8531, Japan*
[7]*Research Institute for Light-induced Acceleration System (RILACS), Osaka Prefecture University, Sakai 599-8531, Japan*
[8]*School of Engineering, Ulster University, Newtownabbey, United Kingdom*

The thermally induced deflection of bimaterial cantilevers was theoretically examined, and an optimal excitation configuration was determined. The optimal heat spot position, resulting in the maximal deflection, was observed at a central location at 0.5–0.6 length for short cantilevers and it shifted backwards the clamped position at 0.4 length for long cantilevers. The calculated values and recent experimental results are in good agreement. The study also confirms indirectly the high value of the convection coefficient for liquid on vibrating surfaces in another experiment. These results can help to determine an optimal detection configuration for chemical and biosensing applications.

The application of bimaterial cantilevers in the metrology of atomic force microscopy has been of interest in several fields of biochemistry[1–3] and physics.[4–10] These measurements rely on the response of cantilevers under various effects due to the environment in which the sample or molecules are immersed.[4,11] Samples, such as virus molecules or bacteria, can be attached to or adsorbed on the cantilever surface and change the cantilever dynamics, as shown in Fig. 1(a). Furthermore, adsorption can increase the effective mass of the cantilever and reduce the resonance frequency.[12] Several effects related to the variations in surface physical properties can arise, for example, the change in surface tension or stress[13] can result in a change in the Young's modulus and alter the frequency. In a recent study,[14] a bending-induced frequency shift was also observed. The thickness of the coating of these cantilevers, which is important in

*Corresponding author email: nguyenduyvy@tdtu.edu.vn

enhancing the sensitivity, was recently determined. Lai *et al.*[8] experimentally demonstrated that the optimal coating-to-substrate thickness ratio the for Al-$SiN_x$ cantilever is 0.26 and that for the Au-$SiN_x$ case is 0.25, while for the former cantilever Liu and Wang reported a higher ratio of $\simeq 0.6$.[15] Recently, Huy *et al.*[16] considered the size effects of thin metallic layers and theoretically concluded to similar results as Lai *et al.*[8]

However, the deflection behaviour depending on the heat absorption is complicated in the sense that the location of adsorption, $x_0$, is arbitrary in an ambient environment; thus, different $x_0$ values can result in a same deflection. This results in the same detected value for the photodetector and reduces the sensitivity of the cantilever. Nevertheless, in most of the studies an excitation is applied at the cantilever end to examine the sensitivity.[7,17] Therefore, determining an optimal acting configuration for the cantilever depending on the excitation position is important. Ramos *et al.*[18] thermally excited a cantilever and demonstrated that the first mode had the greatest amplitude for $x_0 \simeq 0.2L$, where $L$ is the cantilever length. Nevertheless, the greatest deflection was obtained by Voiculescu *et al.*,[4] when the heat source

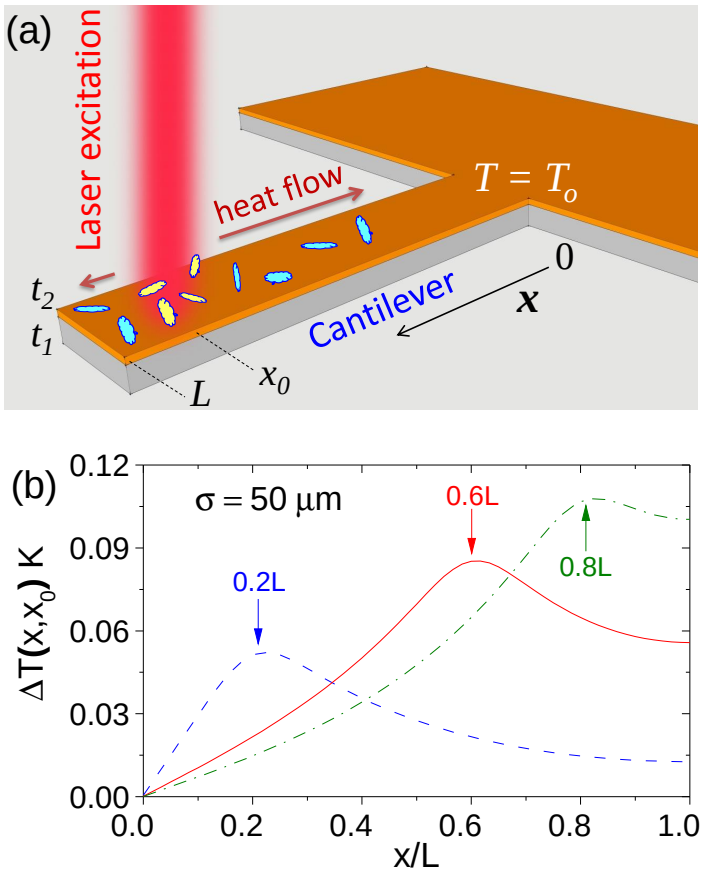


**Fig. 1.** (a) Model of a bimaterial cantilever with adsorbed bio-objects. Infra-red excitation can be used to excite and detect the density of bio-object and the thermal-related phenomena. (b) Temperature distribution at various heat locations, $x_0 = 0.2$–$0.8L$. Here, the thickness of the Au coating is $t_2 = 50$ nm, the beam waist is $\sigma = 50\ \mu\text{m} = 0.1L$, and an absorbed heat of 10 $\mu$W are used.

was positioned at the centre of an Au-coated cantilever. Therefore, the identification of the optimal position for thermal excitation is crucial for chemo/biosensing.

In this study, we determined the dependence of the cantilever response on its dimensions and on the excitation configurations, such as the position and magnitude of the applied heat. The optimal excitation was determined as a function of the cantilever length and it was compared with the experimental results where applicable. These results can provide important information on the control of cantilever response. For example, when the cantilever is excited by infrared radiation, the deflection is proportional to the infrared absorption of the bacteria[19] or cells.[20] In this study, the laser beam was assumed to have an intensity profile of a Gaussian distribution. A special case of a Dirac delta distribution profile has been studied experimentally[1,7] and theoretically.[21]

The heat absorbed by the cantilever due to laser irradiation can be calculated by[14,22]

$$P_{abs} = \int dz |E(z)|^2 \mathbf{Im}[1 - \epsilon(\omega_{opt})]\omega_{opt}/c, \tag{1}$$

where the integration is taken over the coating thickness $t_2$ [see Fig. 1] and $P_{abs}$ over layer $t_1$ is assumed to be negligible. $E(z)$ is the electric field inside the film, $\omega_{opt} = 2\pi c/\lambda$ is the optical frequency of the laser, and $c$ is the speed of light. $\epsilon$ is the complex dielectric function of metallic layer, $\epsilon(\omega_{opt}) = \epsilon_b - \omega_{pl}^2/(\omega_{opt}^2 + i\gamma\omega_{opt})$, where $\epsilon_b$ is the background dielectric constant, $\omega_{pl}$ is the bulk plasma frequency, and $\gamma$ is the nonradiative damping parameter. This absorption is approximately 7% for a 40-nm Au film and reduces to 6.5% [6%] when the thickness increases to 50 [60] nm at a He-Ne laser wavelength of $\lambda = 632.82$ nm.[14]

From position $x_0$, this heat is dispersed to other parts of the cantilever and to the external environment via convection. To simplify the analysis, the following assumptions were applied:

- The heat is quickly transferred over the cantilever thickness, $t_2$ through $t_1$; therefore, there is a uniform heat distribution over the cantilever thickness. This was justified in a recent study where the difference in temperatures between the top and the bottom surfaces is less than 20 $\mu$K for the irradiation by a 10-$\mu$W laser source.[23]

- Heat convection is uniform over the cantilever surface, that is, the convection is independent of $T(x)$.

The one-dimensional temperature distribution, $T(x)$, along the cantilever length ($x = 0$ at the clamped position, shown in Fig. 1(a)) can be written as[17,21]

$$\frac{d^2T(x)}{dx^2} - m^2[T(x) - T(x=0)] + \kappa I(x) = 0, \tag{2}$$

where $m^2 = 2\overline{h}/(k_1t_1 + k_2t_2)$ and $\kappa = \alpha/(k_1t_1 + k_2t_2)$. $t_i[k_i]$ is the thickness[thermal conductivity] of the layer $i$th, $i = 1$ for the silicon substrate and $i = 2$ for the metallic coating. $\alpha$ is the absorption coefficient and $I(x)$ is the laser intensity distribution. The laser beam also exerts a radiation pressure on the cantilever, resulting from the momenta of the photon stream.[24,25]

Nevertheless, this pressure is negligible in comparison to the photothermal effect, as reported in a recent study.[14] In a multilayer system, the optical field acting on the cantilever can be significantly enhanced, and the radiation pressure effect needs to be considered as well. This can be used to vary the relative vibration amplitude of different modes.[26]

The heat spot profile, which is assumed to be a Gaussian function with a beam waist $\sigma$ and centered at $x = x_0$, can be written as

$$I(x) = \beta\Big[\frac{1}{\sigma\sqrt{\pi}}e^{-\frac{(x-x_0)^2}{\sigma^2}}\Big], \tag{3}$$

where $\beta$ is the laser intensity. In the case of $\sigma \simeq 0$, the solution of Eq. (2) is

$$\Delta T(x) = -\frac{\alpha P}{(k_1t_1 + k_2t_2)w\mathbf{erf}(\sqrt{2})}\times \times \begin{cases} \mathrm{Bsinh}\, mx \text{ for } x < x_0, \\ \mathrm{Ccosh}\, mx + \mathrm{Dsinh}\, mx \text{ for } x > x_0. \end{cases} \tag{4}$$

This thermal distribution has been reported in our recent works.[21] Nevertheless, this condition is not alway satisfied when $x_0$ is located in the centre of the cantilever and the thermal conductivity of the coating layer is high, especially when the beam waist [$\sigma \simeq 0.1L$–$0.4L$, see Eq. (3)] is considered. A part of the laser beam misses the cantilever, if $x_0$ is located close to the cantilever end. Therefore, to maintain the same absorbed heat a correction needs to be applied, for example,

$$I(x) = \frac{P}{w.\mathrm{erf}(\sqrt{2})}\left[\frac{1}{\sigma\sqrt{\pi}}e^{-\frac{(x-x_0)^2}{\sigma^2}}\right]. \tag{5}$$

Here, the error function $\mathrm{erf}(x) = (2/\sqrt{\pi})\int_0^x e^{-t^2}dt$ is used to compensate the missed energy and $P$ is the input power of laser.

Using the Gaussian-distributed profile of $I(x)$ to solve Eq. (2), we obtain

$$T(x) - T_0 = -\beta\frac{\mathrm{Exp}[-m(x+x_0) - \frac{L^2+x_0^2}{\sigma^2}]}{4m\sqrt{\pi}\sigma\overline{h}w(1+e^{2Lm})}\Big\{2e^{m(L+x_0)+2Lx_0/\sigma^2}(e^{2mx}-1)m^2 + F\Big\} \tag{6}$$

$$F = e^{(L^2+x_0^2)/\sigma^2 + m^2\sigma^2/4}\sqrt{\pi}\sigma\overline{h}wY$$

$$Y = (1-e^{2mx})\Big[e^{2mx_0}\mathrm{erf}(\frac{L-x_0}{\sigma} - \frac{m\sigma}{2}) + e^{2mL}\mathrm{erf}(\frac{L-x_0}{\sigma} + \frac{m\sigma}{2})\Big] + (1+e^{2mL})\Big[e^{2mx_0}\mathrm{erf}(\frac{-x+x_0}{\sigma} + \frac{m\sigma}{2}) + e^{2mx}\mathrm{erf}(\frac{x-x_0}{\sigma} + \frac{m\sigma}{2})\Big] + (e^{2mx}+e^{2mL})\Big[e^{2mx_0}\mathrm{erf}(\frac{x_0}{\sigma} + \frac{m\sigma}{2}) - \mathrm{erf}(\frac{-x_0}{\sigma} + \frac{m\sigma}{2})\Big]. \tag{7}$$

In Fig. 1(b), $\Delta T = T(x) - T(0)$ is shown with a beam waist of $\sigma = 50\ \mu\mathrm{m} = 0.1L$ where $x_0$ is indicated by arrows. Empirically, the deflection $z(L)$ is the greatest when $x_0$ is located close to the cantilever end. Nevertheless, $z(L)$ presents an involved change versus $x_0$ as it is the accumulation of all deflection elements $dz(x)$ along $L$.

Using the Euler beam theory for bending,[17] the deflection can be written as

$$\frac{d^2z(x)}{dx^2} = N[T(x) - T_0], \tag{8}$$

where $N = 6(\gamma_1 - \gamma_2)(t_1 + t_2)/(t_2^2 K)$,

$$K = 4 + 6\frac{t_1}{t_2} + 4\left(\frac{t_1}{t_2}\right)^2 + \frac{E_1}{E_2}\left(\frac{t_1}{t_2}\right)^3 + \frac{E_2}{E_1}\frac{t_2}{t_1}, \tag{9}$$

and $E_{1[2]}$ is the Young's modulus of the substrate[coating] layer. In the simple case, where the laser intensity is assumed to be a delta function, that is $\sigma \simeq 0$, an analytical form of $z(x)$ can be obtained.[21] Otherwise, the Gaussian form of $I(x)$ in Eq. (3) gives rise to a lengthy formula of Eq. (2). As a result, the analytical solution of Eq. (8) is challenging to obtain and a numerical procedure needs to be employed.

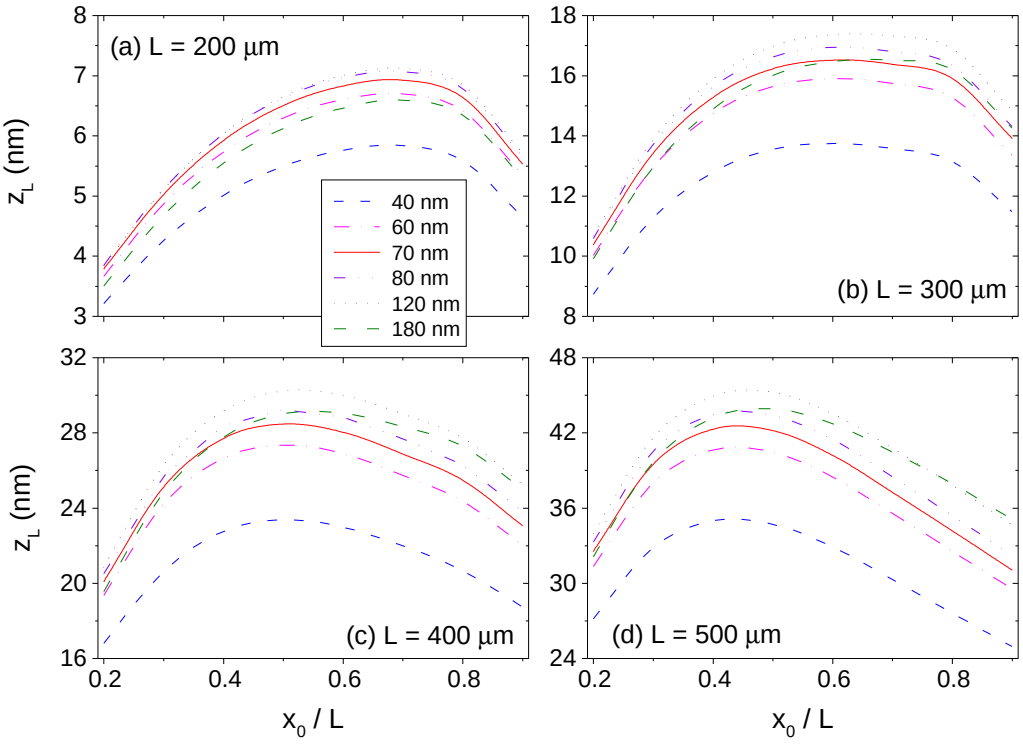


**Fig. 2.** Deflection depending on $x_0$ with four cantilever lengths, $L$. For long cantilevers, the optimum position of the heat source to maximise $z_L$ shifts towards the clamped position, for example, $0.4L$ for $L = 500$ $\mu$m (d). The further parameters are the same as those of Ramos *et al.*[18] for comparison: the cantilever width is $w = 100$ $\mu$m and thickness is $t_1 = 0.9$ $\mu$m.

The thermal distribution around $x$, $T(x)$, is the superposition of the heat flows from the heat source centered at $x_0$ and the wave reflected back from the boundary at $L$. The maximal deflection $z(L)$ is the summation of all deflected element $dz$. As a result, there is an optimum

value of $x_0$ that maximises $z(L)$. As shown in Fig. 2 for Au-coated cantilevers, the involved behaviour of $z(L)$ can be considered as follows.

- As $z(L)$ increases with the increase in $t_2$, it reaches an optimum value at $t_2 = 120$ nm (black dotted lines in Fig. 2), and then decreases. This is due to the nonmonotonic thickness-dependent deflection discussed in Ref.,[16] resulting from the size effects due to the mechanical rigidity and thermal conductivity of the metallic film.
- There is an optimum value of $x_0$ that maximises $z(L)$. For example, $x_0 \simeq 0.6L$ [Fig. 2(a)] for 200- and $\simeq 0.4L$ [Fig. 2(d)] for a 500-$\mu$m long cantilever, respectively.
- The longer the cantilever is, the optimum position shifts closer towards the clamped position: $x_0/L$ decreases from 0.6, to 0.55, 0.45, and 0.4 for $L = 200$, 300, 400, and 500 $\mu$m, respectively.

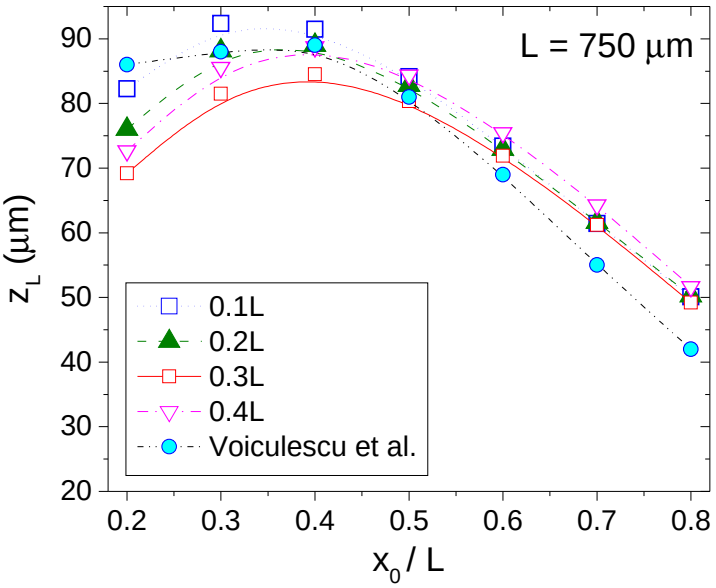


**Fig. 3.** Calculated $z(L)$ values as a function of beam waist, $\sigma = 0.1$–$0.4L$. From experimental results by Voiculescu *et al.*[4] (cyan circles), $\sigma = 0.1L$–$0.2L$ can be obtained. Here $t_2 = t_{Au} = 100$ nm.

In particular, the response depending on $L$ is confirmed where the greatest $z(L)$ is observed at $x_0 \sim 0.1L$–$0.4L$ for long cantilevers, as shown in Fig. 3 together with the experimental results by Voiculescu *et al.*[4] (cyan circles) summarised in Table I. We can conclude that the heat source distanced at $\simeq 15$ $\mu$m from the cantilever in this experiment resulted in a $\sigma$ with a width of $0.1L$–$0.2L$. Although $z(L)$ was measured in liquids, the deflection behaviour is similar because $z(L)$ here corresponds to the detected amplitude of the 1st mode in Ref.[4]

In a recent experiment, Ramos *et al.*[18] examined the response of a 200-$\mu$m long cantilever and obtained the optimal peak located close to the clamped position [indicated by cyan circles,

**Table I.** Calculated deflection, $z_L$ ($\mu$m).

| Heat spot size | Spot position ($x_0/L$) | | | | | | |
|---|---|---|---|---|---|---|---|
| ($\sigma/L$) | 0.2 | 0.3 | 0.4 | 0.5 | 0.6 | 0.7 | 0.8 |
| 0.1 | 82 | 92 | 91 | 84 | 73 | 61 | 50 |
| 0.2 | 76 | 88 | 89 | 83 | 73 | 61 | 50 |
| 0.3 | 69 | 82 | 85 | 80 | 72 | 61 | 49 |
| 0.4 | 72 | 86 | 89 | 84 | 75 | 57 | 52 |
| (*)Ref.[4] | 86 | - | 89 | 81 | 69 | - | 42 |

(*) Heat source is located at 15 $\mu$m distance from the cantilever and $L = 750$ $\mu$m. $\sigma$ could be approximately deduced.

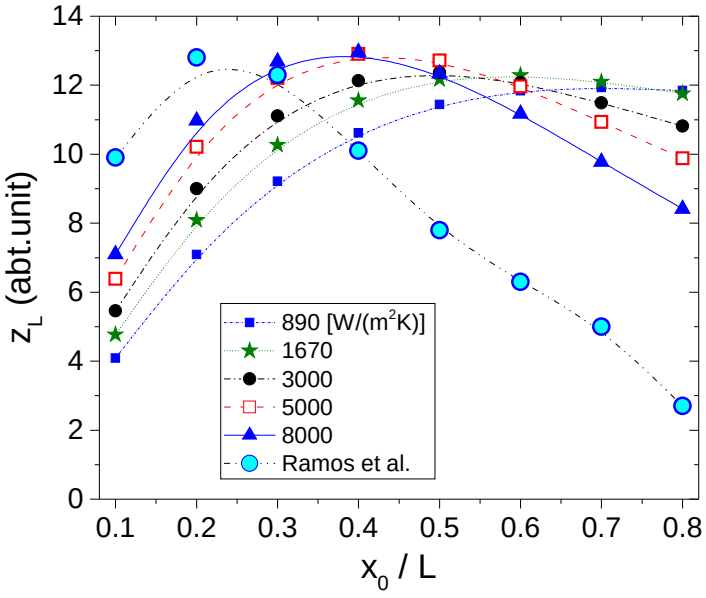


**Fig. 4.** Calculated $z(L)$ values using various convection coefficients, $h = 890$–$8000$ W/(m$^2$K) and experimental results from Ramos *et al.*[18] (cyan circles). The spot size was fixed at $0.1L = 20$ $\mu$m.

dash-dot-dotted line in Fig. 4]. This result can be qualitatively explained if the vibration-dependent heat transfer is considered. It has been shown that vibrating surfaces[27] or liquid[28] can greatly enhance heat transfer; for example, an increase by eight times for Ti films vibrating in water was observed at frequency of kHz in comparison to that for a static film.[27] Therefore, the forced convection can be increased several times and it can result in a different response of the cantilever. In Fig. 4, assuming a high value for the convection coefficient $h$ in the range of 890–8000 W/(m$^2$K), the peaks of $z_L$ can shift towards the clamped direction, $x_0 \rightarrow$

$0.3L$. Nevertheless, these peaks are still located in a closer position to the clamped end and have wider widths than those reported by Ramos *et al.*. More detailed studies are needed to further explain the fast diminishing of $z_L$, that is $z(L) = 0$ at $x_0 = 0.8L$ (last cyan circles) and $0.9L$ (not shown), which implies that there is no response under excitation, contrary to our calculated values. A dynamical analysis can further clarify the experimental results.

In conclusion, using appropriate irradiating configurations, a cantilever length-dependent maximal response was observed and the largest deflection was obtained for a certain position of the heat source. For a long cantilever (e.g., length 500 $\mu$m), this position decreases to approximately 0.4 of the length, which is in agreement with a recent experimental result. For cantilevers shorter than 300 $\mu$m, the spot position located at approximately 0.4–0.6 of the length results in an optimal excitation. Especially, considering the vibration-dependent convection can provide explanation for the experimentally optimal value of the spot position at $0.2L$–$0.3L$.

**Acknowledgment** This research is funded by Vietnam National Foundation for Science and Technology Development (NAFOSTED) under grant number 103.01-2019.345.

## References


1) G. C. Ratcliff and D. A. Erie, Appl. Phys. Lett. **72**, 1911, (1998).
2) S. Kim, D. Lee, X. Liu, C. Van Neste, S. Jeon, and T. Thundat, Sci. Rep. **3**, 1111 (2013).
3) F. Huber, H. P. Lang, J. Zhang, D. Rimoldi, and C. Gerber, Swiss Med Wkly. **145**, 1 (2015).
4) I. Voiculescu, F. Liu, T. Ono, and M. Toda, Sens. Actuator A-Phys. **242**, 58 (2016).
5) N. D. Vy, L. Tri Dat, and T. Iida, Appl. Phys. Lett. **109**, 054102 (2016).
6) S. Hiroshima, A. Yoshinaka, T. Arie, and S. Akita, Jpn. J. Appl. Phys. **52**, 06GH02 (2013).
7) M. Toda, T. Ono, F. Liu, and I. Voiculescu, Rev. Sci. Instrum. **81**, 055104 (2010).
8) J. Lai, T. Perazzo, Z. Shi, and A. Majumdar, Sens. Actuator A-Phys. **58**, 113 (1997).
9) M. C. LeMieux, M. E. McConney, Y.-H. Lin, S. Singamaneni, H. Jiang, T. J. Bunning, and V. V. Tsukruk, Nano Lett. **6**, 730 (2006).
10) S. Singamaneni, M. LeMieux, H. Lang, C. Gerber, Y. Lam, S. Zauscher, P. Datskos, N. Lavrik, H. Jiang, R. Naik, T. Bunning, and V. Tsukruk, Adv. Mater. **20**, 653 (2008).
11) M. F. Khan and N. Miriyala and J. Lee and M. Hassanpourfard and A. Kumar and T. Thundat, Appl. Phys. Lett. **108**, 211906, (2016).
12) B. Labedz, A. Wanczyk, and Z. Rajfur, PLOS ONE **12**(11), 1 (2017).
13) S. Huang and X. Zhang, J. Micromech. Microeng. **17**, 1211 (2007).
14) N. D. Vy and T. Iida, Appl. Phys. Express **9**, 126601 (2016).
15) B. Liu and X. Wang, Int. J. Therm. Sci. **79**, 60 (2014).
16) H. T. Huy, L. T. Dat, and N. D. Vy, J. Appl. Phys. **122**, 224502 (2017).
17) J. R. Barnes, R. J. Stephenson, C. N. Woodburn, S. J. OShea, M. E. Welland, T. Rayment, J. K. Gimzewski, and C. Gerber, Rev. Sci. Instrum. **65**, 3793 (1994).
18) D. Ramos and J. Tamayo and J. Mertens and M. Calleja, J. Appl. Phys. **99**, 124904 (2006).
19) H. Etayash, M. F. Khan, K. Kaur, and T. Thundat, Nat. Commun. **7**, 12947 (2016)
20) N. Inomata, M. Toda, , and T. Ono, Int. J. Automation Tech. **12**, 15 (2018).
21) H. T. Huy, L. T. Dat, and N. D. Vy, Commun. in Phys. **28**(3), 255 (2018).
22) C. M. Hoang, T. Iida, L. T. Dat, H. T. Huy, and N. D. Vy, Opt. Commun. **403**, 150 (2017).
23) D. R. Evans, P. Tayati, H. An, P. K. Lam, V. S. J. Craig, and T. J. Senden, Sci. Rep. **4**, 5567 (2014).
24) N. Duy Vy and T. Iida, Appl. Phys. Lett. **102**, 091101 (2013).
25) N. D. Vy and T. Iida, Appl. Phys. Express **8**, 032801 (2015).
26) C. M. Hoang, N. D. Vy, L. T. Dat, and T. Iida, Jpn. J. Appl. Phys. **56**, 06GK05 (2017).
27) S. W. Wong and W. Y. Chon, AIChE Journal **15**, 281 (1969).
28) S. K. Mishra, H. Chandra, and A. Arora, Int. Nano Lett. **9**, 245 (2019)